an electric field is created in the fissure, which is proportional to the frequency.[3]

Since the parameters involved in the contamination problem are very uncertain, estimations of the magnitude of losses must be crude. However, it can be seen for reasonable values of layer thickness and a conductivity $\sigma \approx 1-100\ (\Omega\, m)^{-1}$, which is representative for semiconductors, that the order of magnitude of the calculated residual losses agrees with those measured. In addition, for reasonable values of layer thickness (1 μ) and size (10 μ) of fissures in the surface, it can be shown that an electric field perpendicular to the surface can create losses which are of the same order of magnitude as, or one order of magnitude higher than, those coming from the fissuring. This is in agreement with measurements.[2]

However, the model has a number of unsolved questions. Thus, the structure and composition of the contamination material are unknown. Furthermore, it is not known how the proximity effect influences the microwave losses in the lossy material.

The author wishes to thank Professor Dr. K. Saermark for the excellent conditions at his department, Physics Laboratory I, The Technical University of Denmark, where the experiments were performed.

[1]P. Kneisel, O. Stoltz, and J. Halbritter, IEEE Trans. Nucl. Sci. NS-18, 159 (1971).
[2]P. Flécher, J. Halbritter, R. Hietschold, P. Kneisel, W. Kühn, and O. Stoltz, IEEE Trans. Nucl. Sci. NS-16, 1018 (1969).
[3]J. Halbritter, J. Appl. Phys. 42, 82 (1971).
[4]J. P. Turneaure and I. Weissman, J. Appl. Phys. 39, 4417 (1968).
[5]J. Halbritter and K. Hoffman, Kernforschungzentrum Karlsruhe Report No. 3/67-9, 1967 (unpublished).
[6]J. M. Pierce, Ph.D. thesis (Stanford University, Stanford, Calif., 1967) (unpublished).
[7]M. Danielsen, Ph.D. thesis (The Technical University of Denmark, 1971) (unpublished).
[8]H. Hahn, H.J. Halama, and E.H. Foster, J. Appl. Phys. 39, 2606 (1968).
[9]H. Hahn and H.J. Halama, IEEE Trans. Nucl. Sci. NS-16, 1013 (1969).
[10]J. P. Turneaure and N. Tuong Viet, Appl. Phys. Letters 16, 333 (1970).
[11]H. Hahn and H.J. Halama, *Proceedings of the 7th International Conference on High Energy Accelerators in Yerevan* (Publishing House of the Academy of Science of the Armenian SSR, 1969), Vol. 2, p. 674.

High-efficiency $Ga_{1-x}Al_xAs$-GaAs solar cells

J.M. Woodall and H.J. Hovel
IBM Thomas J. Watson Research Center, Yorktown Heights, New York 10598
(Received 5 July 1972)

Heterojunction solar cells consisting of $p\mathrm{Ga}_{1-x}\mathrm{Al}_x\mathrm{As}$-$p$GaAs-$n$GaAs are grown by liquid-phase epitaxy and exhibit power conversion efficiencies of over 16% (corrected for contact area) measured in sunlight for air mass 1 at sea level, while efficiencies of 19–20% are obtained for an air mass value of 2 or more. The improved efficiencies compared to conventional homojunction (Si and GaAs) cells are attributed to the reduction of series resistance and the reduction of surface recombination losses resulting from the presence of the heavily doped $Ga_{1-x}Al_xAs$ layer. Open-circuit voltages of 0.98–1.0 V and short-circuit currents of 18–21 mA/cm^2 (corrected for contact area) are observed for a solar input intensity of 98.3 mW/cm^2.

The $Ga_{1-x}Al_xAs$-GaAs heterojunction system is probably unique among heterojunctions in that very few interface states are expected to exist at the boundary between the two materials because of their extremely close lattice match, while at the same time a growth technique is available that is capable of producing high-quality single-crystal material of controlled doping level. The use of a $Ga_{1-x}Al_xAs$ layer on a GaAs substrate is therefore very attractive for solar-cell applications since the layer can be made thick and heavily doped to reduce the series resistance, will be transparent to most wavelengths which are absorbed efficiently by the GaAs, and should greatly reduce the recombination velocity at the GaAs "surface" (i.e., the interface between the two materials). It is the surface recombination velocity which is the greatest cause of low power conversion efficiencies in conventional GaAs solar cells.

The heterojunction cells reported here are grown by liquid-phase epitaxy in a vertical growth system described previously[1]; preliminary electrical measurements on similar cells have also been described.[2] An n-type GaAs wafer doped with Si to a level of $(2-5)\times 10^{17}$ cm^{-3} is placed in a recess located in a carbon substrate holder. A melt consisting of Ga, Al, GaAs chunks, and Zn is placed in a melt chamber adjacent to the wafer; the temperature of the apparatus is then brought to 900 °C in an atmosphere of hydrogen and held constant for a period of 1 h to allow all parts of the system to equilibrate. Initially, the substrate is entirely enclosed by the high-purity carbon to prevent an appreciable loss of As from the surface during the equilibrating period. At the end of this period, the substrate is rotated into position below the melt, and the system is cooled from 900 to 890 °C at a rate of 0.1 °C/min. At 890 °C the sample is rotated away from the melt, and the near equality of the substrate thickness to the depth of the recess in the carbon holder causes the melt to be wiped off the substrate surface, which prevents spurious growth when the sample is cooled down to room temperature.

The Al content of the melt was varied to obtain compositions in the grown layer of $x=0.3$, 0.5, and 0.7,

TABLE I. Values for cell 287-2. Area = 0.1008 cm^2; contact area = 6.3%.

Date	P_{in} (mW/cm^2)	Air mass value	V_{oc} (V)	J_{sc} (mA/cm^2)	P_{out} (mW/cm^2)	η (unc) (%)	η (corr) (%)
28 June 1972	74 ± 2	2.0	0.955	19.5	14.06 ± 0.03	19.1 ± 0.5	20.3 ± 0.6
28 July 1972	85.5 ± 1.4	1.5	0.965	21.2	14.14 ± 0.03	16.3 ± 0.3	17.4 ± 0.3
5 August 1972	98.3 ± 0.5	1.0	0.965	21.3	15.05 ± 0.03	15.3 ± 0.1	16.3 ± 0.1

although most of the cells have been constructed with $x = 0.7$, since of the three the greatest portion of the solar spectrum is utilized for that composition. The thickness of the $Ga_{1-x}Al_xAs$ layer ranges from 6 μ for the $x = 0.7$ composition to 13 μ for the $x = 0.3$ value, and the Zn component in the melt dopes the layer to a range of $(1-4) \times 10^{18}$ cm^{-3}. During the growth period, Zn also diffuses into the *n*GaAs substrate, forming a GaAs *p-n* junction with a junction depth of 0.5–7 μ beneath the interface between the two materials; the junction depth is controlled by varying the Zn content in the melt. To ensure negligible contact resistance between the $Ga_{1-x}Al_xAs$ and the metal contact, a short Zn diffusion is performed before contacting, using $ZnAs_2$ in a closed ampoule at 720 °C for 10–20 min, which raises the Zn surface concentration to greater than 10^{19} cm^{-3}. The devices are made by depositing a crosshatched grid pattern of metallic contacts on the $Ga_{1-x}Al_xAs$, using electroless plating of Au-Zn and electroplating of In, then mounting on TO-5 headers and etching with HCl and H_3PO_4-HNO_3 to reduce the reverse leakage currents to the order of 1 nA. Finally, a SiO coating of about 750-Å thickness is evaporated onto the mounted device to minimize reflection from the surface.

The open-circuit voltage, short-circuit current, and maximum power output of the cells were measured in bright sunlight on cloudless days at near sea-level elevation and at 60–85 °F. The maximum power output was obtained by varying the load resistance across the device terminals and finding the peak value of V^2/R, where V is the output voltage and R is the load resistance. The solar power input to the cells was measured using Eppley Pyroheliometers (thermopiles); the solar input ranged from 69 mW/cm^2, on a cloudless but "hazy" day in which the air mass value (a term which describes the degree of atmospheric absorption[3]) probably exceeded 2, to 98.3 mW/cm^2 on a clear cloudless day with an air mass value of 1.

The efficiencies (power out/power in) of these cells are considerably higher than those previously reported for Si or GaAs homojunction[4,5] and $p$$Ga_{1-x}Al_xAs$-$n$GaAs heterojunction[6] solar cells. Tables I and II list the date of measurement, the power input P_{in}, the approximate air mass value,[3] the open-circuit voltage V_{oc}, the short-circuit current J_{sc} (corrected for contact area), the power output P_{out}, and the efficiency η (both uncorrected and corrected for contact area) for two high-efficiency cells; the junction depth (width of the *p*GaAs region) for these cells was 0.8 μ, and the $Ga_{1-x}Al_xAs$ layer thickness and composition were 6 μ and $x = 0.7$, respectively. At air mass 1, with minimum atmospheric absorption and the sun near the zenith, the cell output ranges from 14 to 15 mW/cm^2 and the corresponding uncorrected efficiencies range from around 14.5 to 15.5%. The efficiencies after correction for contact area are from 15 to over 16%. At air mass 2, the cell output ranges from 13 to 14 mW/cm^2, while the input has decreased from 98 to around 70; the uncorrected efficiencies then range from 18 to 19%, and the corrected values from 19 to over 20%. For comparison, a high-efficiency commercial Si solar cell (Centralab N220CG) was measured under the same conditions; the uncorrected and corrected efficiencies were 10.9 and 11.2% at air mass 1, and 13.2 and 13.6% at air mass 2. Six other growths were made with junction depths between 0.5 and 1.0 μ, using the same $Ga_{1-x}Al_xAs$ thickness and composition. The open-circuit voltages for these ranged from 0.942 to 1.002 V, the short-circuit currents (corrected for contact area) ranged from 17.0 to 21.3 mA/cm^2, and the efficiencies (corrected) ranged from 13.5 to 15.0% at air mass 1, 17 to 19% at air mass 2. The largest cell made with efficiencies in this range had an area of 0.149 cm^2.

It is evident from Tables I and II that solar-cell efficiencies depend strongly on the atmospheric conditions during the measurement, due to both absorption and scattering of the light. The main cause of absorption is water vapor; its effect is to absorb much of the infrared portion of the solar spectrum, leaving the visible portion of the spectrum relatively unattenuated. Since the cells are sensitive mainly in the visible region, the power output does not decrease as rapidly with increasing atmospheric absorption as the power input, and the efficiency therefore increases with increasing air mass value. The same dependence on atmospheric conditions occurs with conventional Si and GaAs solar cells.

Scattering of the solar radiation causes a certain portion of the light incident on the cell to emanate from regions of the hemisphere other than in the direction of the sun.[7,8] This does not affect the measurement of power output from the cells (accuracy ± 0.1%), but it does affect the accuracy of the measurement of power input, since the active elements of the Eppley thermopiles are

TABLE II. Values for cell 288-2. Area = 0.146 cm^2; contact area = 5.45%.

Date	P_{in} (mW/cm^2)	Air mass value	V_{oc} (V)	J_{sc} (mA/cm^2)	P_{out} (mW/cm^2)	η (unc) (%)	η (corr) (%)
28 June 1972	69 ± 2.1	2.1	0.956	17.6	13.0 ± 0.03	18.8 ± 0.6	19.9 ± 0.7
28 July 1972	86.5 ± 1.4	1.5	0.969	19.1	13.5 ± 0.03	15.6 ± 0.3	16.5 ± 0.3
5 August 1972	98.3 ± 0.5	1.0	0.970	19.3	14.12 ± 0.03	14.4 ± 0.1	15.2 ± 0.1

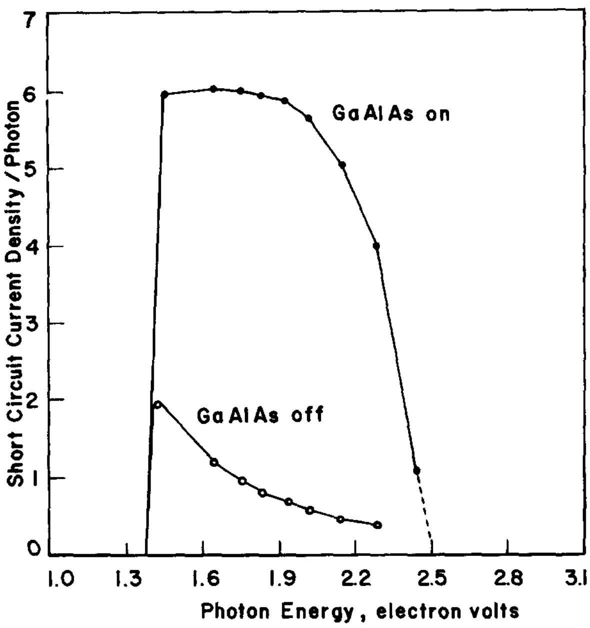

FIG. 1. Spectral response of a 6.7-μ-deep GaAs p-n junction before and after removal of the $Ga_{1-x}Al_xAs$ layer (no antireflective coating). $Ga_{1-x}Al_xAs$ thickness and composition are 6.5 μ and $x = 0.7$, respectively.

recessed and they only record radiation from about one-third of the sky. At air mass 1, virtually all the incident radiation is present in a cone with an apex angle of about 40°,[7,8] and the thermopile records about 99% of the total input power. To account for this, the measured power input at air mass 1 was increased by 1% and an estimated accuracy of ±0.5% was established. The scattering increases with increasing air mass[8]; therefore, the input readings were increased by 3% at air mass 1.5 with an estimated accuracy of ±1.5%, and increased by 6% at air mass 2 with an estimated accuracy of ±3%. These estimates agreed well with the thermopile output as it was pointed in various directions of the sky, as long as the sky did not contain any significant number of clouds (< 5–10%). Clouds behave as reflecting surfaces and greatly reduce the accuracy of the power input measurement.

The higher efficiency of the heterojunction cells compared to conventional GaAs solar cells is attributed to reduced series resistance and to a reduction in the surface recombination velocity at the GaAs p-n junction surface, which enhances the collection efficiency (ratio of the hole-electron pairs separated by the junction to the total number generated by the light). The increased collection efficiency can be seen in Fig. 1, which shows the spectral response of a cell with a 6.7-μ base width before and after removal of the $Ga_{1-x}Al_xAs$ layer by etching in HCl. The peak response of the GaAs p-n junction by itself is low since most of the carriers generated near the surface recombine before they can be collected. The response is considerably higher before the $Ga_{1-x}Al_xAs$ layer is removed, indicating that the effective diffusion length, which includes the effects of both surface and bulk recombination, is greater in the heterojunction case. In addition, the loss of photocarriers by surface recombination causes the response of a GaAs cell without the upper layer to decrease with increasing photon energy because of generation of the carriers closer to the surface as the absorption coefficient increases. The response of the heterojunction cell, on the other hand, is nearly constant up to the point where absorption in the $Ga_{1-x}Al_xAs$ layer begins, indicating that surface recombination is not playing an important role in the heterojunction device.

The authors would like to express their appreciation to R.M. Potemski, A. Benoric, and S. Renick for their technical assistance in portions of this work. They would also like to thank W. Howard for many helpful suggestions concerning fabrication and measurement of the cells, N. Braslau for discussions on atmospheric conditions, and Miss B. Chider and J. D. Kuptsis for the electron-beam microprobe analyses.

[1]J.M. Woodall, J. Crystal Growth 12, 32 (1972).

[2]J.M. Woodall and H.J. Hovel, Electrochemical Society Meeting, Houston, 1972 (unpublished).

[3]P. Moon, J. Franklin Inst. 230, 583 (1940). Air mass is actually defined as the ratio of the path length of radiation through the atmosphere to the path length at the zenith, and Moon's calculations assume an average amount of various impurity species in the atmosphere in calculating the power received at the earth's surface for various air masses. In this letter the optical path is constant, since all measurements are made around noontime, and the amounts of impurities are variable according to the weather conditions. The air mass values given here are found by comparing the input power with Moon's calculated values.

[4]M. Wolf, Proc. IRE 48, 1246 (1960).

[5]A.R. Gobat, M.F. Lamorte, and G.W. McIver, IRE Trans. Military Electron. 6, 20 (1962).

[6]Zh.I. Alferov, V.M. Andreev, M.B. Kagan, I.I. Protasov, and V.G. Trofim, Sov. Phys. Semicond. 4, 2047 (1971).

[7]J.V. Dave and J. Gazdag, Appl. Opt. 9, 1457 (1970).

[8]N. Braslau (private communication).